

Evolution of entropy at small x

G.R.Boroun*

Physics Department, Razi University, Kermanshah 67149, Iran

Phuoc Ha†

Department of Physics, Astronomy and Geosciences, Towson University, Towson, MD 21252

(Dated: February 20, 2025)

We explore the evolution of the Deep Inelastic Scattering (DIS) entropy, defined as $S(x, \mu^2) \simeq \ln[xg(x, \mu^2)]$ at small Bjorken variable x , where μ is the observable scale and the gluon distribution $xg(x, \mu^2)$ is derived from the Dokshitzer-Gribov-Lipatov-Altarelli-Parisi (DGLAP) evolution equations. We aim to evolve the DIS entropy, which is not directly observable, using a Laplace transform technique. This approach allows us to obtain an analytical solution for the DIS entropy based on known initial gluon distribution functions. We consider both leading-order (LO) and higher-order approximations for the DIS entropy, incorporating the evolved gluon distribution function at the initial scale. The DIS entropy, influenced by purely gluonic emissions, varies with higher-order corrections in the running coupling. By comparing predictions with charged hadron multiplicity data, we are able to define the evolution. Additionally, we investigate the derivative of the scaling entropy as a model dependent on the running coupling to determine the parameter λ , the Pomeron intercept. We find that the values of $\lambda(x, \mu^2)$ decrease as the order of evolution increases, which is consistent with the Balitsky-Fadin-Kuraev-Lipatov (BFKL) Pomeron in the LO and NLO approximations. This investigation provides insights into the dynamics of Quantum Chromodynamics (QCD) at high energies.

INTRODUCTION

Entropy, which is an important quantity of a system in thermodynamics, can be described according to the Boltzmann entropy¹ relation $S = k_B \ln W$, where W denotes the number of microstates that correspond to the same macroscopic thermodynamic state, or the Gibbs entropy² relation $S = -k_B \sum p_i \ln p_i$, where p_i gives the probability to find the system in the state $|i\rangle$ [1, 2]. In Deep inelastic Scattering (DIS), at high-energy interaction, the interaction time between the virtual photon and the proton is in general much shorter than the characteristic time scale $t_n \sim 1/E_n$. Indeed, the probe to read off the information about the phases ϕ_n of the individual Fock states $|n\rangle$ with n partons in high-energy interaction is impossible and it causes the resulting information scrambling [3]. The mixed state produced from the proton after the DIS measurement is due to the uncertainty relation between the phase and the occupation number of the Fock states where determine the entropy of the multi-hadron state created in DIS. The entropy of the partons in a DIS experiment resolved by the authors in Refs.[4, 5] by the following form

$$S_{\text{DIS}} = \ln N(x, \mu^2), \quad (1)$$

where $N(x, \mu^2)$ is the number of partons in a hadron with longitudinal light-front momentum fraction x of the struck parton in the target hadron and the observable scale μ can be identified with the proton virtuality $\mu^2 = Q^2$ in the DIS measurement where $q^2 = -Q^2$ is the momentum transfer [6]. $N(x, \mu^2)$, which represents the number of degrees of freedom in the DIS measurement, is defined as the total number of partons per $\ln 1/x$ for the universal entanglement entropy. The entanglement entropy is suggested to be

$$S(x, \mu^2) = \ln N(x, \mu^2), \quad (2)$$

*Electronic address: boroun@razi.ac.ir

†pdha@towson.edu

¹ The Boltzmann entropy describes the disorder or complexity of the system at the microscopic level.

² The Gibbs entropy turns into the Boltzmann entropy if all the microstates have the same probability.

where

$$N(x, \mu^2) \equiv x\Sigma(x, \mu^2) + xg(x, \mu^2), \quad (3)$$

with

$$x\Sigma(x, \mu^2) = \sum_f \left(q_f(x, \mu^2) + \bar{q}_f(x, \mu^2) \right), \quad (4)$$

where $g(x, \mu^2)$ and $q_f(x, \mu^2)$ denote the parton densities of the gluon and the quark of flavor f , respectively. As an alternative, the partonic entropy model has been extended in Refs.[4, 5, 7] based on the dipole entropy and the von Neumann entropy at small x , respectively.

In this paper, we consider the evolution of the DIS entropy at small x , defined by the following form

$$S(x, \mu^2) \simeq \ln \left[xg(x, \mu^2) \right], \quad (5)$$

where the μ -dependent gluon distribution is obtained from the Dokshitzer-Gribov-Lipatov-Altarelli-Parisi (DGLAP) evolution equations [8–10]. We wish to evolve the DIS entropy, which is not a directly observable quantity, using a Laplace transform technique. This allows us to obtain an analytical method for the solution of the DIS entropy in terms of known initial gluon distribution functions. We consider both leading-order (LO) and higher-order approximations for the DIS entropy, incorporating the evolved gluon distribution function at the initial scale. The DIS entropy is based on the treatment of purely gluonic emissions, which naturally increase and decrease with higher-order corrections in the running coupling. By comparing predictions with data for charged hadron multiplicities, one can clearly define the evolution.

In the following, the scaling entropy determines the parameter λ , which is the hard Pomeron intercept. In saturation physics, the parameter λ predicts the transverse momentum-dependent gluon distribution, which grows rapidly as $\sim x^{-\lambda}$. In the DIS entropy, various corrections are employed to extract $\lambda(x, Q^2)$ at higher-order corrections, considering its dependence on x at small x . We investigate the derivative of the scaling entropy as a model dependent on the running coupling to determine the parameter $\lambda(x, Q^2)$, offering a perspective on the dynamics of QCD at high energies.

The paper is organized as follows: in Sec. II, using the Laplace transform technique, we show the evolution of both leading-order (LO) and higher-order approximations for the DIS entropy, incorporating the evolved gluon distribution function at the initial scale. Our results of the gluon entropy, evaluated in this work based on the parametrization groups, and the investigation of the derivative of the scaling entropy as a model dependent on the running coupling to determine the parameter λ , the Pomeron intercept, are presented in Sec. III. Conclusions are given in Sec. IV. A sample calculation of a term that contributes to the DIS entropy at the LO approximation is relegated to Appendix.

EVOLUTION

At small x where the gluon density is dominant, the DGLAP evolution equation for the DIS entropy is defined by the following form

$$\frac{\partial[\exp(S(x, \mu^2))]}{\partial \ln \mu^2} \simeq \int_x^1 \frac{x}{y^2} \left[\frac{\alpha_s}{4\pi} P_{gg}^{\text{LO}}\left(\frac{x}{y}\right) + \left(\frac{\alpha_s}{4\pi}\right)^2 P_{gg}^{\text{NLO}}\left(\frac{x}{y}\right) + \left(\frac{\alpha_s}{4\pi}\right)^3 P_{gg}^{\text{NNLO}}\left(\frac{x}{y}\right) + \dots \right] \exp(S(y, \mu^2)) dy, \quad (6)$$

where the splitting functions are defined in Ref.[11]. The running coupling, in the renormalization group equation (RGE) reads

$$\mu^2 \frac{d\alpha_s(\mu^2)}{d\mu^2} = - \left(b_0 \alpha_s^2(\mu^2) + b_1 \alpha_s^3(\mu^2) + b_2 \alpha_s^4(\mu^2) + \dots \right) \quad (7)$$

where $b_0 = \frac{33-2n_f}{12\pi}$ is referred to as the 1-loop β -function coefficient, the 2-loop coefficient is $b_1 = \frac{153-19n_f}{24\pi^2}$, and the 3-loop coefficient is $b_2 = \frac{2857 - \frac{5033}{9}n_f + \frac{325}{27}n_f^2}{128\pi^3}$ for the SU(3) color group. In the color dipole model [12], the photon wave function depends on the mass of the quarks in the $q\bar{q}$ dipole. Therefore, contributions depend on the mass of the quarks by modifying the Bjorken variable x in the DIS entropy $x \rightarrow \tilde{x}_f \equiv x(1 + 4m_c^2/\mu^2)$ with $m_c = 1.29_{-0.053}^{+0.077}$ GeV where the uncertainties are obtained through adding the experimental fit, model and parametrization uncertainties

in quadrature [13, 14].

We use the method developed in detail in Refs.[15–20] to obtain the evolution [21] of the DIS entropy using a Laplace-transform method by rewriting the variables into $v = \ln(1/x)$ and μ instead of x and μ . The evolution of the DIS entropy, by using the notation $\widehat{S}(v, \mu^2) \equiv S(e^{-v}, \mu^2)$, is

$$\frac{\partial[\exp(\widehat{S}(v, \mu^2))]}{\partial \ln \mu^2} \simeq \int_0^v e^{-(v-w)} \left[\frac{\alpha_s}{4\pi} \widehat{P}_{gg}^{\text{LO}}(v-w) + \left(\frac{\alpha_s}{4\pi}\right)^2 \widehat{P}_{gg}^{\text{NLO}}(v-w) + \left(\frac{\alpha_s}{4\pi}\right)^3 \widehat{P}_{gg}^{\text{NNLO}}(v-w) + \dots \right] \exp(\widehat{S}(w, \mu^2)) dw. \quad (8)$$

Applying the notation that the Laplace transform of the DIS entropy $\widehat{S}(v, \mu^2)$ is given by $\mathcal{S}(s, \mu^2)$ as $\mathcal{S}(s, \mu^2) \equiv \mathcal{L}[\widehat{S}(v, \mu^2); s]$ and using the fact that the Laplace transform of a convolution is simply the ordinary product of the Laplace transforms of the factors, we have

$$\mathcal{L} \left[\int_0^v e^{\widehat{S}(w, \mu^2)} \widehat{H}(v-w, \alpha_s(\mu^2)) dw; s \right] = e^{\mathcal{S}(s, \mu^2)} \times h(s, \alpha_s(\mu^2)), \quad (9)$$

where

$$\begin{aligned} h(s, \alpha_s(\mu^2)) &\equiv \mathcal{L} \left[e^{-v} \left\{ \frac{\alpha_s(\mu^2)}{4\pi} \widehat{P}_{gg}^{\text{LO}}(v) + \left(\frac{\alpha_s(\mu^2)}{4\pi}\right)^2 \widehat{P}_{gg}^{\text{NLO}}(v) + \left(\frac{\alpha_s(\mu^2)}{4\pi}\right)^3 \widehat{P}_{gg}^{\text{NNLO}}(v) + \dots \right\}; s \right] \\ &= \frac{\alpha_s(\mu^2)}{4\pi} h^{(0)}(s) + \left(\frac{\alpha_s(\mu^2)}{4\pi}\right)^2 h^{(1)}(s) + \left(\frac{\alpha_s(\mu^2)}{4\pi}\right)^3 h^{(2)}(s) + \dots \end{aligned} \quad (10)$$

We find that the Laplace transform of the evolution of the DIS entropy is given by

$$\mathcal{S}(s, \mu^2) = \mathcal{S}(s, \mu_0^2) + \frac{h^{(0)}(s)}{4\pi} \int_{\mu_0^2}^{\mu^2} \alpha_s(\tau^2) d\ln \tau^2 + \frac{h^{(1)}(s)}{(4\pi)^2} \int_{\mu_0^2}^{\mu^2} \alpha_s^2(\tau^2) d\ln \tau^2 + \frac{h^{(2)}(s)}{(4\pi)^3} \int_{\mu_0^2}^{\mu^2} \alpha_s^3(\tau^2) d\ln \tau^2 + \dots \quad (11)$$

To simplify the above equation at the leading-order (LO) approximation, we rewrite Eq. (11) as

$$\mathcal{S}^{\text{LO}}(s, \mu^2) = \mathcal{S}^{\text{LO}}(s, \mu_0^2) + \frac{h^{(0)}(s)}{4\pi} \int_{\mu_0^2}^{\mu^2} \alpha_s(\tau^2) d\ln \tau^2, \quad (12)$$

whose coefficient $h^{(0)}(s)$ is given by

$$h^{(0)}(s) = \frac{33 - 2n_f}{3} + 12 \left(\frac{1}{s} - \frac{2}{s+1} + \frac{1}{s+2} - \frac{1}{s+3} - \Psi(s+1) - \gamma_E \right), \quad (13)$$

where the $\Psi(s)$ is defined by $\Psi(s) = \frac{d}{ds} \ln \Gamma(s)$ and $\gamma_E = 0.577216$ is the Euler-Mascheroni constant. The inverse Laplace transform of the coefficients is straightforward and defined by the kernel $\widehat{J}(v, \mu^2) \equiv \mathcal{L}^{-1}[\mathcal{S}(s, \mu^2); v]$. Using the convolution theorem, we find that

$$\widehat{S}(v, \mu^2) = \widehat{S}(v, \mu_0^2) + \frac{1}{4\pi} \int_0^v \widehat{J}(v-w) \left[\int_{\mu_0^2}^{\mu^2} \alpha_s(\tau^2) d\ln \tau^2 \right] dw, \quad (14)$$

where $\widehat{J}(v)$ is defined by

$$\widehat{J}(v) \equiv \mathcal{L}^{-1}[h^{(0)}(s); v] = \left(\frac{33 - 2n_f}{3} \right) \delta(v) + 12 \left[1 - 2e^{-v} + e^{-2v} - e^{-3v} + \frac{1}{2} e^{-v} [1 + \coth(\frac{1}{2}v)] - \gamma_E \delta(v) \right]. \quad (15)$$

Transforming back into x space is straightforward (a sample calculation of the term involving $e^{-v} \coth(\frac{1}{2}v)$ is provided in the Appendix). Therefore, the DIS entropy, depending on the initial conditions, at the LO approximation is given by

$$S^{\text{LO}}(x, \mu^2) = S^{\text{LO}}(x, \mu_0^2) + \frac{P^{(0)}(x)}{4\pi} \int_{\mu_0^2}^{\mu^2} \alpha_s(\tau^2) d\ln \tau^2, \quad (16)$$

where

$$P^{(0)}(x) = \left(\frac{33 - 2n_f}{3} \right) + \left[12 \ln \frac{1-x}{x} - 22 + 24x - 6x^2 + 4x^3 - 12\gamma_E \right]. \quad (17)$$

The DIS entropy at the initial gluon distribution in the scale μ_0^2 is defined by the following form

$$S(x, \mu_0^2) \simeq \ln \left[xg(x, \mu_0^2) \right]. \quad (18)$$

Usually, parametrization groups (such as the CT18 [22], MSTW [23], JR09 [24] and NNPDF [25, 26] collaborations) use the following form for the gluon distribution function at the initial scale μ_0^2 as

$$xg(x, \mu_0^2) = A_g x^{\delta_g} (1-x)^{\eta_g} p_g(y(x)), \quad (19)$$

where p_g is a functional form that is widely used in PDF sets where the input $y(x)$ differs between them and is replaced by a neural network $NN_g(x)$ [25, 26].

The evolution of the DIS entropy at the next-to-leading-order approximation (NLO) is defined by

$$\mathcal{S}(s, \mu^2) = \mathcal{S}(s, \mu_0^2) + \frac{h^{(0)}(s)}{4\pi} \int_{\mu_0^2}^{\mu^2} \alpha_s(\tau^2) d\ln\tau^2 + \frac{h^{(1)}(s)}{(4\pi)^2} \int_{\mu_0^2}^{\mu^2} \alpha_s^2(\tau^2) d\ln\tau^2, \quad (20)$$

where the coefficient of $h^{(1)}(s)$ is derived completely in s -space by authors in Ref. [27]. We keep the largest terms in the limit $s \rightarrow 0$, then we have

$$h^{(1)}(s)|_{s \rightarrow 0} \simeq \left(\frac{4}{3} C_F T_f - \frac{46}{9} C_A T_f \right) \frac{1}{s} - (C_A^2 \ln(16)) \frac{1}{s^2}, \quad (21)$$

with $C_F = \frac{N_c^2 - 1}{2N_c}$, $C_A = N_c$, $T_R = \frac{1}{2}$, and $T_f = T_R n_f$ for the SU(3) values of C_A and C_F , where the n_f is the number of active quark flavors. The inverse Laplace transform of the entropy at the NLO approximation is found as

$$\widehat{S}(v, \mu^2) \simeq \widehat{S}(v, \mu_0^2) + \frac{1}{4\pi} \int_0^v \widehat{J}(v-w) \left[\int_{\mu_0^2}^{\mu^2} \alpha_s(\tau^2) d\ln\tau^2 \right] dw + \frac{1}{(4\pi)^2} \int_0^v \widehat{\eta}(v-w) \left[\int_{\mu_0^2}^{\mu^2} \alpha_s^2(\tau^2) d\ln\tau^2 \right] dw, \quad (22)$$

where $\widehat{\eta}(v)$ is defined by

$$\widehat{\eta}(v) \equiv \mathcal{L}^{-1}[h^{(1)}(s); v] = \left(\frac{4}{3} C_F T_f - \frac{46}{9} C_A T_f \right) - (C_A^2 \ln(16)) v. \quad (23)$$

Therefore, the DIS entropy at the NLO approximation is given by

$$S^{\text{NLO}}(x, \mu^2) = S^{\text{NLO}}(x, \mu_0^2) + \frac{P^{(0)}(x)}{4\pi} \int_{\mu_0^2}^{\mu^2} \alpha_s(\tau^2) d\ln\tau^2 + \frac{P^{(1)}(x)}{(4\pi)^2} \int_{\mu_0^2}^{\mu^2} \alpha_s^2(\tau^2) d\ln\tau^2, \quad (24)$$

where

$$P^{(1)}(x) = \left(\frac{4}{3} C_F T_f - \frac{46}{9} C_A T_f \right) \ln \frac{1}{x} - (C_A^2 \ln(16)) \left(\ln \frac{1}{x} \right)^2, \quad (25)$$

and

$$S^{\text{NLO}}(x, \mu_0^2) \simeq \ln \left[xg^{\text{NLO}}(x, \mu_0^2) \right]. \quad (26)$$

At small x , we return to the end-point behavior of the three-loop gluon-gluon splitting function in s -space as

$$h^{(2)}(s)|_{s \rightarrow 0} \simeq -\frac{E_1}{s^2} + \frac{E_2}{s}, \quad (27)$$

where $E_1 \simeq 2675.85 + 157.269n_f$ and $E_2 \simeq 14214.2 + 182.958n_f - 2.79853n_f^2$ [11]. The inverse Laplace transform of the coefficients $h^{(2)}(s)$ is straightforward, as

$$\widehat{\gamma}(v) \equiv \mathcal{L}^{-1}[h^{(2)}(s); v] = -E_1 v + E_2. \quad (28)$$

Now, we find that

$$\begin{aligned} \widehat{S}(v, \mu^2) &\simeq \widehat{S}(v, \mu_0^2) + \frac{1}{4\pi} \int_0^v \widehat{J}(v-w) \left[\int_{\mu_0^2}^{\mu^2} \alpha_s(\tau^2) d\ln\tau^2 \right] dw + \frac{1}{(4\pi)^2} \int_0^v \widehat{\eta}(v-w) \left[\int_{\mu_0^2}^{\mu^2} \alpha_s^2(\tau^2) d\ln\tau^2 \right] dw \\ &+ \frac{1}{(4\pi)^3} \int_0^v \widehat{\gamma}(v-w) \left[\int_{\mu_0^2}^{\mu^2} \alpha_s^3(\tau^2) d\ln\tau^2 \right] dw. \end{aligned} \quad (29)$$

Therefore, the DIS entropy at the next-to-next-to-leading-order approximation (NNLO) is given by

$$\begin{aligned} S^{\text{NNLO}}(x, \mu^2) &= S^{\text{NNLO}}(x, \mu_0^2) + \frac{P^{(0)}(x)}{4\pi} \int_{\mu_0^2}^{\mu^2} \alpha_s(\tau^2) d\ln\tau^2 + \frac{P^{(1)}(x)}{(4\pi)^2} \int_{\mu_0^2}^{\mu^2} \alpha_s^2(\tau^2) d\ln\tau^2 \\ &+ \frac{P^{(2)}(x)}{(4\pi)^3} \int_{\mu_0^2}^{\mu^2} \alpha_s^3(\tau^2) d\ln\tau^2, \end{aligned} \quad (30)$$

where

$$P^{(2)}(x) = -E_1 \ln \frac{1}{x} + E_2, \quad (31)$$

and

$$S^{\text{NNLO}}(x, \mu_0^2) \simeq \ln \left[x g^{\text{NNLO}}(x, \mu_0^2) \right]. \quad (32)$$

RESULTS

To predict the entropy at higher-order approximations, it depends on the gluon distribution at the initial scale μ_0^2 and the QCD cut-off Λ . The QCD cut-off parameter in the modified minimal subtraction (MS) scheme [28] is determined using the 4-loop expression for the running of α_s in Ref.[29]. The world average value for $\Lambda_{\overline{\text{MS}}}$ is defined to be

$$\Lambda_{\overline{\text{MS}}}^{n_f=4} = (292 \pm 16) \text{ MeV}, \quad (33)$$

for $n_f = 4$. In this paper, the gluon distributions are used at the initial scales by the following forms:

- The MSTW [23] at the LO approximation at the input scale $\mu_0^2 = 1 \text{ GeV}^2$ (the NLO and NNLO approximations according to Fig.1 are negative at low values of x ($x < 0.01$)). reads

$$xg(x, \mu_0^2) = A_g x^{\delta_g} (1-x)^{\eta_g} [1 + \epsilon_g \sqrt{x} + \gamma_g x] + A_{g'} x^{\delta_{g'}} (1-x)^{\eta_{g'}}. \quad (34)$$

- The CJ15 [30] at the NLO approximation at the input scale $\mu_0 = m_c$ reads

$$xg(x, \mu_0^2) = A_g x^{\delta_g} (1-x)^{\eta_g} [1 + \epsilon_g \sqrt{x} + \gamma_g x], \quad (35)$$

where the charm quark mass is defined as $m_c = 1.29_{-0.053}^{+0.077} \text{ GeV}$ [13, 14].

- The CT18 [22] at the NNLO approximation at the input scale $\mu_0 = 1.3 \text{ GeV}$ reads

$$xg(x, \mu_0^2) = A_g x^{\delta_g-1} (1-x)^{\eta_g} [\sinh(\epsilon_g)(1-\sqrt{x})^3 + \sinh(\gamma_g)3\sqrt{x}(1-\sqrt{x})^2 + (3+2\delta_g)x(1-\sqrt{x}) + x^{3/2}], \quad (36)$$

where the input gluon distribution parameters are given in Table I.

In Fig.1, the gluon distributions based on the parametrization groups (i.e., MSTW [23], CJ15 [30], and CT18 [22]) at the initial scales in a wide range of the Bjorken values of x are plotted. The gluon distributions based on the MSTW [23] at the NLO and NNLO approximations are negative at low values of x . In the following, we used the CJ15 [30] at the NLO approximation and the CT18 [22] at the NNLO approximation.

In Fig.2, a comparison is made between the different evaluations for the gluon entropy at the LO and NLO approximations based on the MSTW and CJ15 respectively. It is plotted as a function of x for virtualities $\mu^2 = 2, 10$ and 100 GeV^2 . Results are shown with and without the rescaling variable as the behavior of evolution of the gluon entropy with the rescaling variable is in line with others.

TABLE I: The parameter values are provided for three parametrization groups.

Parameters	MSTW LO	CJ15 NLO	CT18 NNLO
A_g	0.0012216	45.542	2.690
δ_g	$-0.83657^{+0.15}_{-0.14}$	0.60307 ± 0.031164	0.531
η_g	$2.3882^{+0.51}_{-0.50}$	6.4812 ± 0.96748	3.148
ϵ_g	-38.997^{+36}_{-35}	-3.3064 ± 0.13418	3.032
γ_g	1445.5^{+880}_{-750}	3.1721 ± 0.31376	-1.705
$A_{g'}$	-	-	-
$\delta_{g'}$	-	-	-
$\eta_{g'}$	-	-	-

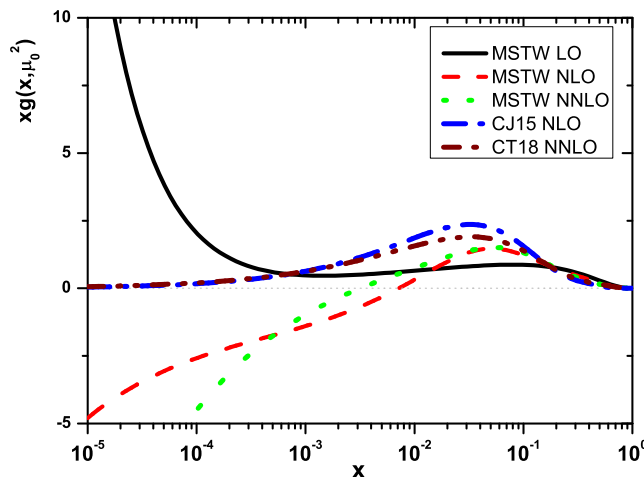


FIG. 1: The gluon distributions at the LO (solid-black), NLO (dashed-red), and NNLO (dot-green) approximations from the MSTW 2008 PDFs [23] at the initial scale $\mu_0 = 1$ GeV, the NLO (dashed-dot-blue) approximation from the CJ15 PDFs [30] at the initial scale $\mu_0 = m_c$ and the NNLO (dashed-dot-dot-brown) approximation from the CT18 PDFs [22] at the initial scale $\mu_0 = 1.3$ GeV, are plotted.

In Fig.3, we show the gluon entropy evaluated in this work based on the parametrization groups. The extracted values are compared with the H1 collaboration data [31] as a function of the average Bjorken $\langle x_{bj} \rangle$ measured in different average squared momentum transfer $\langle \mu^2 \rangle$ ranges, obtained from $\sqrt{s} = 319$ GeV ep collisions. For this dataset, the track pseudorapidities in the hadronic center-of-mass frame are limited to the range $0 < \eta^* < 4$. The H1 data included total errors from statistical and systematic uncertainties. There is a good agreement between the $S(x, \mu^2)$ predicted at the NLO and NNLO approximations and the entropy reconstructed from hadron multiplicity at very small x . The resulting gluonic entropy aligns very well with the hadronic entropy at moderate values of μ^2 .

The authors in Ref.[7] have shown that the estimate of charged versus total hadron multiplicity assumes that the total number of produced hadrons is roughly 3/2 times the number of charged hadrons observed in experiments, as the partonic entropy is defined by

$$S_{\text{Partonic}} \rightarrow S_{\text{Charged}} = S_{\text{Partonic}} + \ln\left(\frac{2}{3}\right). \quad (37)$$

In Table II, we display the charged results at the NLO and NNLO approximations from Eq.(37) and compare them with the H1 hadron entropy derived from multiplicity distributions measured in ep DIS at $\langle \mu^2 \rangle = 30$ GeV² as a function of $\langle x \rangle$. These results show that despite the very small uncertainties in the H1 data, both corrections (i.e., NLO and NNLO) provide very good fits to the data, relating the former to the entropy of final-state hadrons.

It is worth mentioning the pomeron intercept via scaling entropy analysis that has been recently determined in the geometrical scaling properties of the inclusive DIS cross section in Ref.[32]. This intercept is expressed in terms of the scaling entropy obtained from event multiplicities $P(N)$ of final-state hadrons, which is a more efficient way to

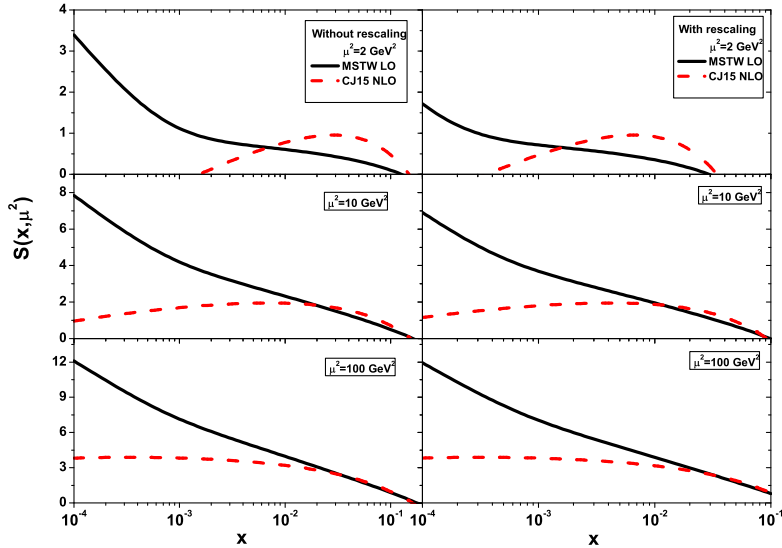


FIG. 2: The evolution of gluonic entropy at $\mu^2 = 2, 10$ and 100 GeV^2 without the rescaling (left diagrams) and with the rescaling (right diagrams) based on the MSTW LO [23] (solid black) and the CJ15 NLO [30] (dashed red).

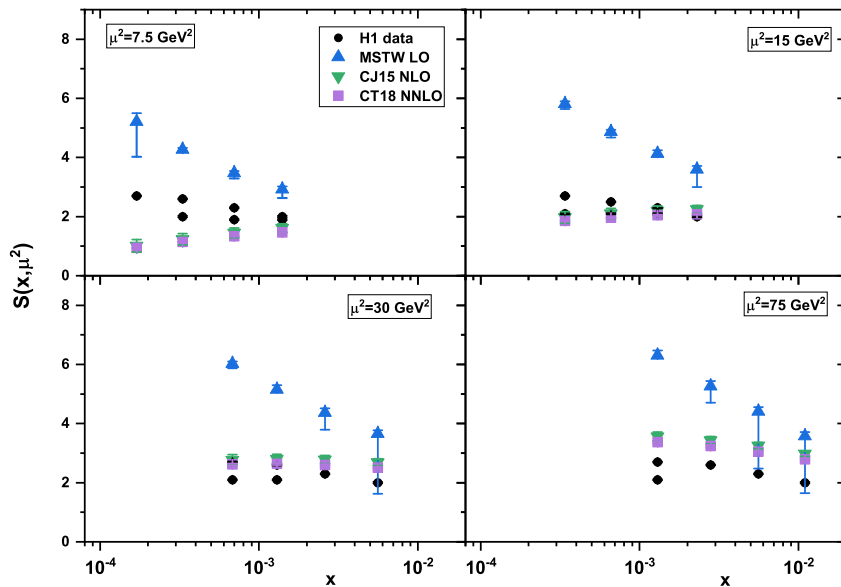


FIG. 3: The evolution of gluon entropy is calculated using the MSTW LO [23] (up triangle), the CJ15 NLO [30] (down triangle), and the CT18 NNLO [22] (squared) and compared with H1 data [31] as a function of x at μ^2 values of $7.5, 15, 30$, and 75 GeV^2 . The H1 collaboration data [31] is presented as a function of $\langle x_{b_j} \rangle$ measured in various averaged μ^2 ranges at $\sqrt{s} = 319 \text{ GeV}$ ep collisions, accompanied by total errors (For this dataset, the track pseudorapidities in the hadronic center-of-mass frame are limited to the range $0 < \eta^* < 4$).

TABLE II: The gluonic entropy, corrected for charged hadrons, is only $\ln[xg] + \ln(\frac{2}{3})$ at $\langle \mu^2 \rangle = 30 \text{ GeV}^2$. This is compared in the NLO and NNLO approximations by the H1 collaboration data [31].

$\langle x \rangle$	NLO	NNLO	H1
0.0052	$2.287^{+0.116}_{-0.114}$	$2.099^{+0.022}_{-0.027}$	2 ± 0.027
0.0026	$2.377^{+0.134}_{-0.133}$	$2.197^{+0.026}_{-0.031}$	2.3 ± 0.021
0.0013	$2.398^{+0.154}_{-0.153}$	$2.229^{+0.028}_{-0.033}$	2.35 ± 0.021
0.00068	$2.389^{+0.173}_{-0.172}$	$2.212^{+0.029}_{-0.034}$	2.4 ± 0.021

detect scaling in experimental data. In the Boltzmann-Gibbs (BG) form, the entropy is given by

$$S(x) = - \int \mathcal{P}(x, k_T) \ln[\mathcal{P}(x, k_T)] d^2 k_T, \quad (38)$$

where $\mathcal{P}(x, k_T)$ is the scattering amplitude in the transverse momentum space. The entropy results, assuming the scaling relation holds, are defined by the following form

$$S = C + \lambda \ln\left(\frac{1}{x}\right). \quad (39)$$

The constant C , due to the power-like gluon distribution, can be estimated into the hadron entropy as defined in Ref.[32]. In multiplicity data (the HERA ep data), the entropy is defined as

$$S^{\text{mult}} = - \sum_N P(N) \ln(P(N)), \quad (40)$$

where $P(N)$ is the probability of detecting N charged hadrons. The authors in Ref.[32] obtained the averaged value of λ by scaling of the partonic entropy at each Q^2 bin (for $\mu^2 = 7.5, 15, 30$ and 70 GeV^2) as

$$\lambda_{\text{entropy}} = 0.322 \pm 0.007. \quad (41)$$

In Fig.4, we show a calculation of the derivative

$$\left(\frac{\partial \ln S(x, \mu^2)}{\partial \ln(1/x)} \right)_{\mu^2} \equiv \lambda(x, \mu^2) \quad (42)$$

of the gluonic entropy $S(x, \mu^2)$ in the low x domain of deeply inelastic ep scattering [33, 34]. The behavior of the determined values of λ is presented due to the MSTW LO [23] (solid-black), the CJ15 NLO [30] (dashed-red), and the CT18 NNLO [22] (dashed dot-green) in Fig.4 at $\mu^2 = 30 \text{ GeV}^2$ without (left diagram) and with (right diagram) correction for charge hadrons (i.e., Eq.(37)), respectively. The curves in a wide range of x are compared by the scaling of the partonic entropy value $\lambda_{\text{entropy}} = 0.322$ [32] (dot-brown), by the inclusive cross section method $\lambda_{\sigma} = 0.329$ [32] (dot-blue) and the bCGC model [35] which gives $\lambda_{\text{bCGC}} \simeq 0.18$ (dot-orange).

The values of λ predicted in the literature are constant as plotted in Fig.4, although $\lambda(x, \mu^2)$ depends on x . Indeed, the evolution of entropy due to the running coupling order is defined by an effective intercept as [34]

$$\frac{\partial \ln S(x, \mu^2)}{\partial \ln(1/x)} = \lambda(x, \mu^2) + \ln\left(\frac{1}{x}\right) \frac{\partial \lambda(x, \mu^2)}{\partial \ln(1/x)}. \quad (43)$$

We observe that, in Fig.4, λ depends on x . Therefore, the effective intercept and x -slope do not coincide. We conclude that one needs to be very careful when considering entropy and its behavior in the small- x region. In particular, at fixed μ^2 and $x \rightarrow 0$, we observe (in Fig.4) a decreasing x -slope and hence $\lambda(x, \mu^2)$ at the LO and higher-order approximations. One can see in Fig.4 that the curve calculated in the LO approximation is close to the theoretical values of λ for $x \leq 10^{-2}$, while the higher-order corrections are noticeably different from those values. We observe that the λ values decrease as the order of evolution increases. The results at the NLO and NNLO approximations decrease as x values decrease. Indeed, such an evolution should lead to a damping of the fast growth of entropy at the higher-order corrections. The estimate of λ at the LO approximation in the interval $10^{-4} \leq x \leq 10^{-2}$ at $\mu^2 = 30 \text{ GeV}^2$ is $\langle \lambda \rangle_{\text{LO}} \simeq 0.28$ without correction for charged hadrons (i.e., Eq.(37)), which is in good agreement with the GBW model [38]. It is $\langle \lambda \rangle_{\text{LO}} \simeq 0.31$ with correction for charged hadrons (i.e., Eq.(37)) in good agreement with the MM

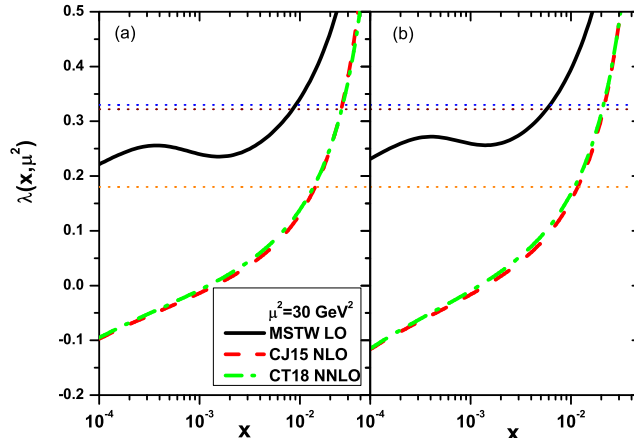


FIG. 4: The values of $\lambda(x, \mu^2)$ are obtained as a function of x at $\mu^2 = 30 \text{ GeV}^2$ using the MSTW LO [23] (solid-black), the CJ15 NLO [30] (dashed-red), and the CT18 NNLO [22] (dashed dot-green) and compared with $\lambda_{\text{entropy}} = 0.322$ [32] (dot-brown), $\lambda_{\sigma} = 0.329$ [32] (dot-blue) and $\lambda_{\text{bCGC}} \simeq 0.18$ [35] (dot-orange) without (left diagram) and with (right diagram) correction for charged hadrons (i.e., Eq.(37)), respectively.

model [32]. The averaged values of λ in Fig.5 are approximately independent of μ^2 in the interval 0.18-0.33 at low values of x . However, the λ values depend on the μ^2 values, both without (left diagram) and with (right diagram) correction for charged hadrons (i.e., Eq.(37)) respectively. As shown, $\lambda(x, Q^2)$ decreases as μ^2 increases. The number of gluons and possibly seaquarks that yield charged hadrons is effective in the λ values obtained from the derivative of the DIS entropy, as illustrated in the right plane of Fig.5. The λ values corrected for charged hadrons (right panel) increase compared to the left panel. This dependence is visible at lower μ^2 values than at higher μ^2 values.

At the same time it seems possible, in principle, to derive some conclusions about the effective intercept from the BFKL at the LO and NLO approximations. The well known Balitsky-Fadin-Kuraev-Lipatov (BFKL) Pomeron in the LO and NLO approximations has defined by the following forms as [36, 37]

$$\lambda_{\text{BFKL}}^{\text{LO}} = \alpha_{IP} - 1 = 12 \ln 2 (\alpha_s / \pi), \quad (44)$$

and

$$\lambda_{\text{BFKL}}^{\text{NLO}} = \alpha_{IP}^{\overline{MS}} - 1 = 12 \ln 2 \frac{\alpha_s}{\pi} [1 + r_{\overline{MS}}(0) \frac{\alpha_s}{\pi}], \quad (45)$$

where $r_{\overline{MS}}(0) \simeq -20.12 - 0.1020n_f + 0.06692\beta_0$ and $\beta_0 = \frac{1}{3}(33 - 2n_f)$. We observe that the NLO BFKL Pomeron intercept for $N_C = 3$ and $n_f = 4$ is calculated to be $\lambda_{\text{BFKL}}^{\text{NLO}} \simeq -0.14$ for $\alpha_s = 0.2$. The results obtained for the entropy with higher-order corrections present an opportunity for utilizing NLO BFKL resummation in high-energy phenomenology.

The λ values in the NLO approximation depend on the μ^2 values, both without (left diagrams) and with (right diagrams) correction for charged hadrons (i.e., Eq.(37)) shown in Fig.6. It is observed that $\lambda(x, \mu^2)$ increases at higher-order corrections as μ^2 increases. The corrected λ values for charged hadrons (right diagram) decrease compared to the uncorrected values (left diagram). This trend is noticeable at lower μ^2 values than at higher μ^2 values. The λ values in the NLO approximation closely resemble $\lambda_{\text{BFKL}}^{\text{NLO}}$ [36, 37] at low μ^2 values and λ_{bCGC} [35] at high μ^2 values.

CONCLUSIONS

We have presented a method based on the Laplace transform to determine the evolution of gluonic entropy at leading-order and higher-order approximations. This method relies on the behavior of the gluon distribution function at initial scales which depends on the running coupling. The gluon distributions at the initial scales are defined based

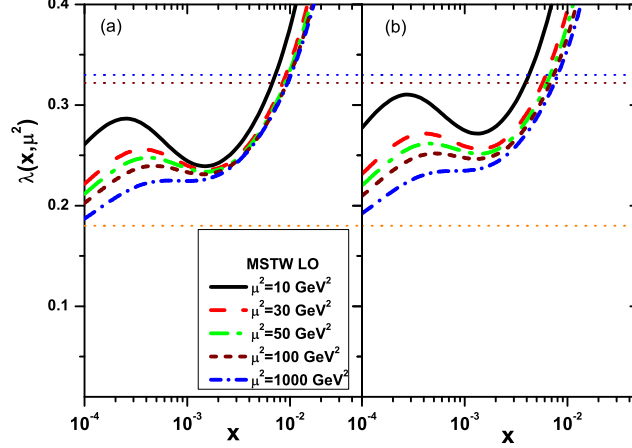


FIG. 5: The values of $\lambda(x, \mu^2)$ are obtained as a function of x in a wide range of μ^2 at the LO approximation. The curves are plotted for $\mu^2 = 10 \text{ GeV}^2$ (solid-black), $\mu^2 = 30 \text{ GeV}^2$ (dashed-red), $\mu^2 = 50 \text{ GeV}^2$ (dashed dot-green), $\mu^2 = 100 \text{ GeV}^2$ (short dashed-brown), and $\mu^2 = 1000 \text{ GeV}^2$ (short dashed dot-blue) without (left diagram) and with (right diagram) correction for charged hadrons (i.e., Eq.(37)), respectively and compared with $\lambda_{\text{entropy}} = 0.322$ [32] (dot-brown), $\lambda_{\sigma} = 0.329$ [32] (dot-blue) and $\lambda_{\text{bCGC}} \simeq 0.18$ [35] (dot-orange).

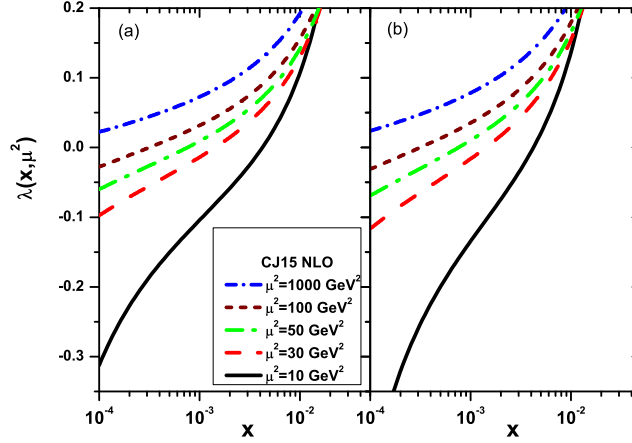


FIG. 6: The values of $\lambda(x, \mu^2)$ are obtained as a function of x in a wide range of μ^2 at the NLO approximation. The curves are plotted for $\mu^2 = 10 \text{ GeV}^2$ (solid-black), $\mu^2 = 30 \text{ GeV}^2$ (dashed-red), $\mu^2 = 50 \text{ GeV}^2$ (dashed dot-green), $\mu^2 = 100 \text{ GeV}^2$ (short dashed-brown), and $\mu^2 = 1000 \text{ GeV}^2$ (short dashed dot-blue) without (left diagram) and with (right diagram) correction for charged hadrons (i.e., Eq.(37)), respectively.

on parametrization groups of MSTW, CJ15, and CT18 at the LO, NLO, and NNLO approximations, respectively. The results of the DIS entropy with the rescaling variable are consistent with the H1 collaboration data reconstructed from hadron multiplicity at small x .

The gluonic entropy shows improvement with respect to the charged hadron effects at the NLO and NNLO approximations compared to the H1 hadron entropy, accompanied by total errors. The Pomeron intercept via scaling entropy is considered and compared with results obtained from event multiplicities $P(N)$ of final-state hadrons. The behavior of $\lambda(x, \mu^2)$ in the evolution of the DIS entropy with respect to the running coupling is examined, showing dependence on x . The values of $\lambda(x, \mu^2)$ decrease as the order of evolution increases, which is consistent with the

BFKL Pomeron in the LO and NLO approximations.

We conclude that the values of $\lambda(x, \mu^2)$ obtained from scaling entropy at the LO approximation fall within the range of results obtained from the bCGC model and the inclusive cross-section of HERA data. We believe that this investigation provides insights into the dynamics of Quantum Chromodynamics (QCD) at high energies.

ACKNOWLEDGMENTS

G.R.Boroun is grateful to Razi University for the financial support provided for this project. Additionally, G.R.Boroun would like to express thanks to Professor K.Kutak for his helpful comments and invaluable support. Phuoc Ha would like to thank Professor Loyal Durand for all his insightful comments and invaluable support.

APPENDIX

Let us consider the integral

$$I = \int_0^v e^{-(v-w)} \coth\left(\frac{1}{2}(v-w)\right) dw. \quad (46)$$

Changing the variable $v - w = u$, then $dw = -du$ and the integral can be written as

$$I = \int_0^v e^{-u} \coth\left(\frac{u}{2}\right) du = \int_0^v e^{-u} \frac{1 + e^{-u}}{(1 - e^{-u})_+} du. \quad (47)$$

In the last term, we set $t = e^{-u}$, $e^{-u} du = -dt$ to get

$$I = \int_x^1 dt \frac{1+t}{(1-t)_+} = \int_x^1 dt \frac{2}{(1-t)_+} - \int_x^1 dt, \quad (48)$$

where $x = e^v$.

Using the definition of the $1/(1-t)_+$ prescription,

$$\int_x^1 dt \frac{f(t)}{(1-t)_+} = \int_x^1 dt \frac{f(t) - f(1)}{1-t} + f(1) \ln(1-x), \quad (49)$$

with $f(t) = 1$, we find

$$I = 2 \ln(1-x) - (1-x). \quad (50)$$

-
- [1] K. Kutak, Phys. Lett. B **705**, 217 (2011); arXiv:1103.3654.
 - [2] R. Wang, arXiv:2208.13151.
 - [3] M.Hentschinski, D.E.Kharzeev, K.Kutak and Z.Tu, arXiv:2408.01259.
 - [4] D. E. Kharzeev and E. M. Levin, Phys.Rev.D **95**, 114008 (2017).
 - [5] D. E. Kharzeev and E. M. Levin, Phys.Rev.D **104**, L031503 (2021).
 - [6] H.G.Dosch, Guy F. de Teramond and S.J.Brodsky, Physics Letters B **850**, 138521 (2024); arXiv:2304.14207.
 - [7] M.Hentschinski, K.Kutak and R.Straka, Eur.Phys. J. C **82** 1147 (2022).
 - [8] Yu.L.Dokshitzer, Sov.Phys.JETP **46**, 641 (1977).
 - [9] G.Altarelli and G.Parisi, Nucl.Phys.B **126**, 298 (1977).
 - [10] V.N.Gribov and L.N.Lipatov, Sov.J.Nucl.Phys. **15**, 438 (1972).
 - [11] A.Vogt, S.Moch and J.A.Vermaseren, Nucl.Phys.B **691**, 129 (2004).
 - [12] N. N. Nikolaev and B. G. Zakharov, Phys. Lett. B **332**, 184 (1994).
 - [13] H1 and ZEUS Collaborations (Abramowicz H. et al.), Eur. Phys. J. C **78**, 473 (2018).
 - [14] H1 Collab. (V.Andreev et al.), Eur.Phys.J.C **74**, 2814 (2014).

- [15] Martin M. Block, Loyal Durand and Douglas W. McKay, Phys.Rev.D **79**, 014031 (2009).
- [16] Martin M. Block, Loyal Durand, Phuoc Ha and Douglas W. McKay, Phys.Rev.D **83**, 054009 (2011).
- [17] Martin M. Block, Loyal Durand, Phuoc Ha and Douglas W. McKay, Phys.Rev.D **84**, 094010 (2011).
- [18] Martin M. Block, Loyal Durand, Phuoc Ha and Douglas W. McKay, Phys.Rev.D **88**, 014006 (2013).
- [19] G.R.Boroun and Phuoc Ha, Phys.Rev.D **109**, 094037 (2024).
- [20] G.R.Boroun and Phuoc Ha, Phys.Rev.D **111**, 034012 (2025).
- [21] G.R.Boroun, Eur.Phys. J. C **84**, 960 (2024).
- [22] T.-J. Hou et al., Phys. Rev. D **103**, 014013 (2021).
- [23] A.D. Martin, W.J. Stirling, R.S. Thorne, G. Watt, Eur. Phys. J. C **63**, 189 (2009).
- [24] P. Jimenez-Delgado, E. Reya, Phys. Rev. D **79**, 074023 (2009).
- [25] S. Carrazza, J. Cruz-Martinez, R. Stegeman, Eur. Phys. J. C **82**, 163 (2022).
- [26] J. Rojo, arXiv:hep-ph/0607122.
- [27] H.Khanpour, A.Mirjalili and S.Atashbar Tehrani, Phys.Rev.C **95**, 035201 (2017).
- [28] W.A. Bardeen et al., Phys. Rev. D **18**, 3998 (1978).
- [29] C. Patrignani et al. (Particle Data Group), Chin. Phys. **C40**, 100001 (2016).
- [30] A. Accardi, L. T. Brady, W. Melnitchouk, J. F. Owens and N. Sato, Phys. Rev. D **93**, 114017 (2016).
- [31] H1 Collab. (V.Andreev , A.Baghdasaryan, A.Baty et al.), Eur. Phys. J. C **81**, 212 (2021).
- [32] L.S.Moriggi and M.V.T.Machado, arXiv [hep-ph]: 2412.16348.
- [33] H1 Collab. (C.Adloff et al.), Phys.Lett.B **520**, 183 (2001).
- [34] P.Desgrolard, A.Lengyel and E.Martynov , JHEP **02**, 029 (2002).
- [35] G. Watt and H. Kowalski, Phys. Rev. D **78**, 014016 (2008).
- [36] V.T.Kim, L.N.Lipatov and G.B.Pivovarov, arXiv [hep-ph]:9911242.
- [37] V.S.Fadin, V.T.Kim, L.N.Lipatov and G.B.Pivovarov, arXiv [hep-ph]:0207296.
- [38] K. J. Golec-Biernat and M. Wusthoff, Phys. Rev. D **59**, 014017 (1998); Phys. Rev. D **60**, 114023 (1999).